

On causal extrapolation of sequences with applications to forecasting*

Nikolai Dokuchaev[†]

November 6, 2018

Abstract

The paper suggests a method of extrapolation of notion of one-sided semi-infinite sequences representing traces of two-sided band-limited sequences; this features ensure uniqueness of this extrapolation and possibility to use this for forecasting. This lead to a forecasting method for more general sequences without this feature based on minimization of the mean square error between the observed path and a predicable sequence. These procedure involves calculation of this predictable path; the procedure can be interpreted as causal smoothing. The corresponding smoothed sequences allow unique extrapolations to future times that can be interpreted as optimal forecasts.

Key words: smooth sequences, extrapolation, frequency analysis, forecasting

AMS 2010 classification: 42A38, 93E10, 42A99

1 Introduction

We study causal dynamic approximation and extrapolation of real sequences in deterministic setting, i.e. without probabilistic assumptions. Extrapolation of sequences can be used for forecasting and was studied intensively, for example, in the framework of system identification methods; see e.g. [23]. In signal processing, there is an approach oriented on the frequency analysis and exploring special features of the band-limited processes such as predictability. For stochastic stationary discrete time processes, the connection between predicability and degeneracy of the spectrum was established by the classical Szegő-Kolmogorov Theorem; see a recent reviews in [4]. This theorem says that the optimal prediction error is zero if its spectral density is vanishing with a certain rate at a point of the unit circle $\mathbb{T} = \{z \in \mathbf{C} : |z| = 1\}$, in particular, if it is vanishing on an arc on \mathbb{T} . In this case, the process is called "band-limited". This result was expanded on more general stochastic processes featuring spectral densities; see, e.g., [8]. In deterministic pathwise setting

*Accepted for publication in Applied Mathematics and Computation

[†]Department of Mathematics & Statistics, Curtin University, GPO Box U1987, Perth, 6845 Western Australia

without probability assumptions, this result was expanded [9, 10] on sequences with Z-transform vanishing at a point of \mathbb{T} .

The present suggests to use the predicability featuring by band-limited processes for forecasting of more general processes that are not necessarily band-limited. This requires calculation of a trace of a band-limited process representing optimal approximation of the available observations. The extrapolation of this trace of a band-limited process can be used as a forecast. The motivation for that approach is based on the assumption that a band-limited part of a process can be interpreted as its regular part purified from a noise represented by high-frequency component. This leads to a problem of causal band-limited approximations for non-bandlimited processes which can be interpreted as a causal band-limited smoothing.

A known two-sided sequence can be converted into a band-limited process with a low-pass filter, and the resulting process will be an optimal band-limited approximation. However, a ideal low-pass filter is non-causal; therefore, it cannot be applied for dynamically observable processes with unavailable future values which excludes predicting and extrapolation problems. Respectively, causal smoothing cannot convert a process into a band-limited one; it is known that the distance of an ideal low-pass filter from the set of all causal filters is positive [3]. There are many works devoted to causal smoothing and sampling, oriented on estimation and minimization of errors in L_2 -norms or similar norms, especially in stochastic setting; see e.g. [1, 2, 3, 6, 7, 9, 10, 13, 16, 19, 20, 25, 27, 28].

The present paper readdresses the problem of causal band-limited smoothing approximation and considers the problem of causal band-limited extrapolation for one-sided real sequences that are not necessary paths of band-limited processes.

We consider purely discrete time processes rather than samples of continuous time processes; one may say that the values between fixed discrete times are not included into consideration. This setting imposes certain restrictions. In particular, it does not allow to consider continuously variable locations of the sampling points, as is common in sampling analysis of continuous time processes; see e.g. [5, 16, 18, 21]. For continuous time processes, the predicting horizon can be selected to be arbitrarily small, such as in the model considered in [5]; this possibility is absent for discrete time processes considered below. In addition, it is not obvious how to define for discrete time processes or sequences an analog of the continuous time analyticity that is often associated with predicability.

Further, we consider the problem in the deterministic setting, i.e. pathwise. This means that the method has to rely on the intrinsic properties of a sole underlying sequence without appealing to statistical properties of an ensemble of sequences. In particular, we use a pathwise optimality criterion rather than criterions calculated via the expectation on a probability space such as mean variance criterions.

In addition, we consider an approximation that does not target the match of the values at any set of selected points; the error is not expected to be small. This is different from a more common

setting where the goal is to match an approximating curve with the underlying process at certain sampling points; see e.g. [7, 18, 19, 21]. Our setting is closer to the setting from [16, 17, 24, 27, 28]. In [16, 17], the point-wise matching error was estimated for a sampling series and for a band-limited process representing smoothed underlying continuous time process; the estimate featured a given vanishing error. In [24], the problem of minimization of the total energy of the approximating bandlimited process was considered; this causal approximation was constructed within a given distance from the original process smoothed by an ideal low-pass filter. Another related result was obtained in [15], where an interpolation problem for absent sampling points was considered in a setting with vanishing error, for a finite number of sampling points. In [27], extrapolation of a trace of a band-limited process from a finite number of points was considered in a frequency setting for a general linear transform and some special Slepian's type basis in the frequency domain. In [28], a setting similar to [27] was considered for extrapolation of a trace of continuous time process from a finite interval using a special basis from eigenfunctions in the frequency domain. Our setting is different: we consider extrapolation without exact match of values for the underlying process. Therefore, we suggest to calculate extrapolations that can be used for forecasting that are not necessarily matching the values of the underlying process. This allows to consider semi-infinite underlying processes that are not paths of band-limited processes.

It can be noted that the framework of two-sided sequences required for detecting of the bandlimitness via Z-transforms are not always convenient to use. For example, consider a situation where the data is collected dynamically during a prolonged time interval. For many models, it is more convenient to represent this data flow as one-sided sequences such that $x(t)$ represents outdated observations with diminishing significance as $t \rightarrow -\infty$. However, application of the two-sided Z-transform requires to select some past time at the middle of the time interval of the observations as the zero point for a model of the two-sided sequence; this could be inconvenient. On the other hand, a straightforward application of the one-sided Z-transform to the historical data represented as one-sided sequences generates Z-transforms that cannot vanish on a part of the unit circle, even for traces of band-limited two-sided sequences. So far, the notion of bandlimitness was not expanded on the one-sided sequences $\{x(t)\}_{t=0,-1,-2,\dots,-\infty}$. The paper addresses this problem, as well as the problem of detecting one-sided semi-infinite sequences that can be extended into two-sided band-limited processes (i.e. representing traces of band-limited processes).

The paper suggests a method of extrapolation of notion of one-sided semi-infinite sequences representing traces of two-sided band-limited sequences; this features ensure uniqueness of this extrapolation and possibility to use this for forecasting. This lead to a forecasting method for more general sequences without this feature based on minimization of the mean square error between the observed path and a predicable sequence. These procedure involves calculation of this predictable path; the procedure can be interpreted as causal smoothing. The corresponding smoothed sequences allow unique extrapolations to future times that can be interpreted as optimal forecasts.

For the solution, we use non-singularity of special sinc matrices obtained in [21] for the solution of the so-called superoscillations problem for continuous time processes; see the references in [18, 21]. It can be noted that the setting in [18, 21] considers exact matching of the band-limited process and the underlying process in certain points, which is different from our setting.

The sustainability of the method is demonstrated with some numerical experiments where we compare the band-limited extrapolation with some classical spline based interpolations.

2 Definitions

We use notation $\text{sinc}(x) = \sin(x)/x$, and we denote by \mathbb{Z} the set of all integers.

We assume that we are given $\Omega \in (0, \pi)$ an a positive integer N . In addition, we are given $s \in \mathbb{Z}$ and $q \in \{k \in \mathbb{Z} : k < s\} \cup \{-\infty\}$.

Let $\mathcal{T} = \{t \in \mathbb{Z} : q \leq t \leq s\}$ if $q > -\infty$ and $\mathcal{T} = \{t \in \mathbb{Z} : t \leq s\}$ if $q = -\infty$.

Let \mathbb{Z}_N be the set of all integers k such that $|k| \leq N$.

For a Hilbert space H , we denote by $(\cdot, \cdot)_H$ the corresponding inner product. We denote by $L_2(D)$ the usual Hilbert space of complex valued square integrable functions $x : D \rightarrow \mathbf{C}$, where D is an interval in \mathbf{R} . We denote by ℓ_r the set of all sequences $x = \{x(t)\}_{t \in \mathbb{Z}} \subset \mathbf{C}$, such that $\|x\|_{\ell_r} = (\sum_{t=-\infty}^{\infty} |x(t)|^r)^{1/r} < +\infty$ for $r \in [1, \infty)$ or $\|x\|_{\ell_\infty} = \sup_t |x(t)| < +\infty$ for $r = +\infty$.

Let ℓ_r^+ be the set of all sequences $x \in \ell_r$ such that $x(t) = 0$ for $t = -1, -2, -3, \dots$; see, e.g. [26].

Let $\mathbb{T} = \{z \in \mathbf{C} : |z| = 1\}$.

For $x \in \ell_1$ or $x \in \ell_2$, we denote by $X = \mathcal{Z}x$ the Z-transform

$$X(z) = \sum_{t=-\infty}^{\infty} x(t)z^{-t}, \quad z \in \mathbb{T}.$$

Respectively, the inverse Z-transform $x = \mathcal{Z}^{-1}X$ is defined as

$$x(t) = \frac{1}{2\pi} \int_{-\pi}^{\pi} X(e^{i\omega}) e^{i\omega t} d\omega, \quad t = 0, \pm 1, \pm 2, \dots$$

If $x \in \ell_2$, then $X|_{\mathbb{T}}$ is defined as an element of $L_2(\mathbb{T})$.

Let $\tau \in \mathbb{Z} \cup \{+\infty\}$ and $\theta < \tau$; the case where $\theta = -\infty$ is not excluded. We denote by $\ell_2(\theta, \tau)$ the Hilbert space of complex valued sequences $\{x(t)\}_{t=\theta}^{\tau}$ such that $\|x\|_{\ell_2(\theta, \tau)} = (\sum_{t=\theta}^{\tau} |x(t)|^2)^{1/2} < +\infty$.

Let \mathcal{Y}_N be the Hilbert space of sequences $\{y_k\}_{k=-N}^N \subset \mathbf{C}$ provided with the ℓ_2 -norm, i.e., $\|y\|_{\mathcal{Y}_N} = (\sum_{k \in \mathbb{Z}_N} |y_k|^2)^{1/2} < +\infty$.

Let ℓ_2^{BL} be the set of all mappings $x \in \ell_2$ such that $X(e^{i\omega}) \in L_2(-\pi, \pi)$ and $X(e^{i\omega}) = 0$ for $|\omega| > \Omega$, where $X = \mathcal{Z}x$. We will call the the corresponding processes $x = \mathcal{Z}^{-1}X$ *band-limited*.

Let \mathbb{B}_N be the set of all $X \in L_2(\mathcal{T})$ such that there exists a sequence $\{y_k\}_{k=-N}^N \in \mathcal{Y}_N$ such that $X(e^{i\omega}) = \sum_{k=-N}^N y_k e^{ik\omega\pi/\Omega} \mathbb{I}_{\{|\omega| \leq \Omega\}}$, where \mathbb{I} is the indicator function.

Consider the Hilbert spaces of sequences $\mathcal{X} = \ell_2$ and $\mathcal{X}_- = \ell_2(q, s)$.

Let B_N be the subset of \mathcal{X}_- consisting of sequences $\{x(t)\}_{t \in \mathcal{T}}$, where $x \in \mathcal{X}$ are such that $x(t) = (\mathcal{Z}^{-1}X)(t)$ for $t \in \mathcal{T}$ for some $X(e^{i\omega}) \in \mathbb{B}_N$.

Definition 2.1. We call an one-sided sequence $x' \in \ell_2(-\infty, s)$ left band-limited if there exists $x \in \ell_2^{BL}$ such that $x(t) = x'(t)$ for $t \leq s$. We denote by $\ell_2^{BL}(-\infty, s)$ the set of all these sequences x' , and we denote by $\ell_{2,N}^{BL}(-\infty, s)$ the set of all these sequences x' such that the corresponding extrapolation x belongs to B_N .

3 Main results

3.1 Uniqueness of the extrapolation for left band-limited processes

Lemma 3.1. (i) For $x_L \in \ell_2^{BL}(-\infty, s)$, the extrapolation $\bar{x} \in \ell_2$ described in Definition 2.1 is uniquely defined.

(ii) If $s - q \geq 2N + 1$, then, for any $x \in B_N$, there exists an unique $X \in \mathbb{B}_N$ such that $x(t) = (\mathcal{Z}^{-1}X)(t)$ for $t \in \mathcal{T}$.

By Lemma 3.1 (i), the future of a band-limited process x is uniquely defined by its history $\{x(t), t \leq s\}$. This statement represent a reformulation in the deterministic setting of the classical Szegő-Kolmogorov Theorem for stationary Gaussian processes [4]. In addition, Lemma 3.1(ii) states that the future of processes from B_N is uniquely defined by a finite set of historical values that has at least $2N + 1$ elements.

Corollary 3.1. (i) If $q > -\infty$ and $s - q \leq 2N + 1$, then $\{x(t)\}_{t \in \mathcal{T}} \in B_N$ for any $x \in \ell_2$.

(ii) If $s - q < 2N + 1$, then there are many $X \in \mathbb{B}_N$ such that $x(t) = (\mathcal{Z}^{-1}X)(t)$ for $t \in \mathcal{T}$; they form a linear manifold in B_N .

3.2 Optimal left band-limited approximation

Let $x \in \mathcal{X}$ be a process. We assume that the sequence $\{x(t)\}_{t \in \mathcal{T}}$ represents available historical data.

Theorem 3.1. (i) There exists an optimal solution \hat{x} of the minimization problem

$$\text{Minimize } \sum_{t=q}^s |\hat{x}(t) - x(t)|^2 \quad \text{over } \hat{x} \in B_N. \quad (1)$$

(ii) If $s - q \geq 2N + 1$, then the corresponding optimal process \hat{x} is uniquely defined.

Under the assumptions of Theorem 3.1(ii), by Lemma 3.1, there exists a unique extrapolation of the band-limited solution \hat{x} of problem (1) on the future times $t > s$. It can be interpreted as the optimal forecast (optimal given Ω and N).

Corollary 3.2. *If $s - q < 2N + 1$ then there are many optimal processes $\hat{x} \in B_N$ such that $\sum_{t=q}^s |\hat{x}(t) - x(t)|^2 = 0$; they form a linear manifold in B_N .*

Up to the end of this section, we assume that the assumptions of Lemma 3.1 and Theorem 3.1(ii) are satisfied.

The optimal solution

Let the operator $\mathcal{Q} : \mathcal{Y}_N \rightarrow B_N$ be defined as $\hat{x} = \mathcal{Q}y = \mathcal{Z}^{-1}\hat{X}$, where

$$\hat{X}(e^{i\omega}) = \sum_{k \in \mathbb{Z}_N} y_k e^{ik\omega\pi/\Omega} \mathbb{I}_{\{|\omega| \leq \Omega\}},$$

for the corresponding $y = \{y_k\} \in \mathcal{Y}_N$. Similarly to the classical sinc representation, we obtain that

$$\begin{aligned} \hat{x}(t) &= \frac{1}{2\pi} \int_{-\Omega}^{\Omega} \left(\sum_{k \in \mathbb{Z}_N} y_k e^{ik\omega\pi/\Omega} \right) e^{i\omega t} d\omega = \frac{1}{2\pi} \sum_{k \in \mathbb{Z}_N} y_k \int_{-\Omega}^{\Omega} e^{ik\omega\pi/\Omega + i\omega t} d\omega \\ &= \frac{1}{2\pi} \sum_{k \in \mathbb{Z}_N} y_k \frac{e^{ik\pi + i\Omega t} - e^{-ik\pi - i\Omega t}}{ik\pi/\Omega + it} = \frac{\Omega}{\pi} \sum_{k \in \mathbb{Z}_N} y_k \text{sinc}(k\pi + \Omega t) = (\mathcal{Q}y)(t). \end{aligned} \quad (2)$$

It follows that the $\mathcal{Q} : \mathcal{Y}_N \rightarrow B_N$ is actually defined as

$$\hat{x}(t) = (\mathcal{Q}y)(t) = \frac{\Omega}{\pi} \sum_{k \in \mathbb{Z}_N} y_k \text{sinc}(k\pi + \Omega t).$$

Consider the operator $\mathcal{Q}^* : B_N \rightarrow \mathcal{Y}_N$ being adjoint to the operator $\mathcal{Q} : \mathcal{Y}_N \rightarrow B_N$, i.e., such that

$$(\mathcal{Q}^*x)_k = \frac{\Omega}{\pi} \sum_{t \in \mathcal{T}} \text{sinc}(k\pi + \Omega t) x(t). \quad (3)$$

By the property of the sinc function, it follows that this convolution maps continuously ℓ_2 into ℓ_2 . Hence the operator \mathcal{Q}^* can be extended as a continuous linear operator $\mathcal{Q}^* : \mathcal{X}_- \rightarrow \mathcal{Y}_N$.

Consider the linear bounded non-negative definite Hermitian operator $R : \mathcal{Y}_N \rightarrow \mathcal{Y}_N$ defined as

$$R = \mathcal{Q}^* \mathcal{Q}.$$

Theorem 3.2. (i) *The operator $R : \mathcal{Y}_N \rightarrow \mathcal{Y}_N$ has a bounded inverse operator $R^{-1} : \mathcal{Y}_N \rightarrow \mathcal{Y}_N$.*

(ii) *Problem (1) has a unique solution*

$$\hat{x} = \mathcal{Q}R^{-1}\mathcal{Q}^*x. \quad (4)$$

Remark 3.1. *It can be noted that $\hat{x} = \mathcal{Q}\mathcal{Q}^+x$, where $\mathcal{Q}^+ = R^{-1}\mathcal{Q}^* : \mathcal{X}_- \rightarrow \mathcal{Y}_N$ is a Moore–Penrose pseudoinverse of the operator $\mathcal{Q} : \mathcal{Y}_N \rightarrow \mathcal{X}_-$.*

Let us elaborate equation (4). The optimal process \hat{x} can be expressed as

$$\hat{x}(t) = \hat{x}(t, q, s) = \frac{\Omega}{\pi} \sum_{k \in \mathbb{Z}_N} \hat{y}_k \text{sinc}(k\pi + \Omega t).$$

Here $\hat{y} = \{\hat{y}_k\}_{k=-N}^N$ is defined as

$$\hat{y} = R^{-1} \mathcal{Q}x. \quad (5)$$

The space \mathcal{Y}_N is finite dimensional, and the operator R can be represented via a matrix $R = \{R_{km}\} \in \mathbf{C}^{2N+1, 2N+1}$, where $k, m = -N, -N+1, \dots, N-1, N$. In this setting, $(Ry)_k = \sum_{m=-N}^N R_{km} y_m$, and the components of the matrix R are defined as

$$R_{km} = \frac{\Omega^2}{\pi^2} \sum_{t=q}^s \text{sinc}(m\pi + \Omega t) \text{sinc}(k\pi + \Omega t).$$

Respectively, the components of the vector $\mathcal{Q}^*x = \{(\mathcal{Q}^*x)_k\}_{k=-N}^N$ are defined as

$$(\mathcal{Q}^*x)_k = \frac{\Omega}{\pi} \sum_{t=q}^s \text{sinc}(k\pi + \Omega t) x(t). \quad (6)$$

Remark 3.2. *The process $\hat{x}(t)$ represents the output of a linear causal smoothing filter. It can be noted that the operators R and \mathcal{Q} have to be recalculated for each s , and the values $\hat{x}(t) = \hat{x}_{q,s}(t)$ calculated for observations $\{x(t), s \leq t \leq q\}$, can be different from the values $\hat{x}_{q,s+\tau}(t)$ calculated for the same t using the observations $\{x(t), s \leq t \leq q + \tau\}$, where $\tau > 0$. Therefore, this filter is not time invariant.*

Remark 3.3. *We have excluded the case where $\Omega = \pi$; this case leads to the trivial solution with $x(-t) = y_t$ for $t \in \mathbb{Z}_N$.*

3.3 Detecting left bandlimitness

Theorem 3.2 allows to verify if $x \in \ell_2(-\infty, s)$ is left band-limited, i.e. if the conditions of Definition 2.1 hold. This can be formulated as the following.

Theorem 3.3. *If $x \in B_N$ then $x \in \ell_{2,N}^{LBL}(-\infty, s)$ if and only if*

$$(x_L, x_L)_{\ell_2(-\infty, s)} = (\mathcal{Q}x_L, R^{-1} \mathcal{Q}x_L)_{\ell_2}.$$

An alternative approach to detection of left bandlimitness was suggested in [14].

3.4 Tikhonov regularization

This let us consider a modification of the original optimization problem (1) with penalty on the norm of the solution that restrains the norm of the solution. More precisely, let us consider the following problem;

$$\text{Minimize } \|\hat{x} - x\|_{\mathcal{X}_-}^2 + \varepsilon \|\hat{x}\|_{\ell_2}^2 \quad \text{over } \hat{x} = B_N, \quad (7)$$

where $\varepsilon > 0$ is a parameter.

Theorem 3.4. *Problem (13) has a unique solution*

$$\hat{x} = \mathcal{Q}R_\varepsilon^{-1}\mathcal{Q}^*x, \quad (8)$$

where

$$R_\varepsilon = R + \varepsilon I,$$

where I is the unit matrix in $\mathbf{R}^{N \times N}$.

Problem (7) can be considered as a regularization of the original optimization problem (1) similarly to the setting from [24]. We found in numerical experiments that, for large N , numerical calculation of inverse matrix R^{-1} is not exact, and the error $E = \|\mathcal{Q}^*x - R\hat{y}\|_{\ell_2(q,s)}$ for a numerical solution \hat{y} of equation (5) does not vanish. It appears that the numerical stability can be improved via this regularization.

In fact, the replacement of R by R_ε may help to decrease the error E even in the original setting. In particular, we observed that, for large N and small $\varepsilon > 0$,

$$\|\mathcal{Q}^*x - R\hat{y}_\varepsilon\|_{\mathcal{X}_-} < \|\mathcal{Q}^*x - R\hat{y}\|_{\mathcal{X}_-}$$

for $y_\varepsilon = R_\varepsilon^{-1}\mathcal{Q}^*x$ and $y = R^{-1}\mathcal{Q}^*x$ such that the optimal solution for problem (3.4) is $\hat{x} = \mathcal{Q}y_\varepsilon$ and the optimal solution for problem (3.2) is $\hat{x} = \mathcal{Q}y$. We observed this, for example, for $N = 200$ and $\varepsilon = 0.05$.

4 Proofs

Proof of Lemma 3.1. Let us prove statement (i). Let $D \triangleq \{z \in \mathbf{C} : |z| < 1\}$. Let $H^2(D)$ be the Hardy space of functions that are holomorphic on D with finite norm $\|h\|_{\mathcal{H}^2(D)} = \sup_{\rho < 1} \|h(\rho e^{i\omega})\|_{L_2(-\pi, \pi)}$. Without a loss of generality, we assume that $s = 0$. In this case, $\mathcal{T} = \{t : t \leq 0\}$. It suffices to prove that if $x \in B_N$ is such that $x(t) = 0$ for $t \leq 0$, then $x(t) = 0$ for $t > 0$. Let $X = \mathcal{Z}x$. Since $x \in B_N$, it follows that $X \in \mathbb{B}_\infty$. We have that $X|_D = (\mathcal{Z}x)|_D \in H^2(D)$. Hence, by the property of the Hardy space, $X \equiv 0$; see, e.g., Theorem

17.18 from [22]. This completes the proof of Lemma 3.1 for $N = +\infty$ and $q = -\infty$. It can be noted that the proof for this case follows also from the predictability of the two-sided band limited processes established in [10, 11].

Let us prove statement (ii). We use an approach based on non-singularity of special sink matrices established in [21]. Without a loss of generality, we assume that $s = N$.

Let us consider first the case when $s - q = 2N + 1$. It suffices to consider $q = -N$ only; in this case, the set $\mathcal{T} = \{t : q \leq t \leq s\} = \{t : -N \leq t \leq N\}$, i.e., $\mathcal{T} = \mathbb{Z}_N$ and it has $2N - 1$ elements. It suffices to prove that if $x(\cdot) \in B_N$ is such that $x(t) = 0$ for $t \in \mathcal{T}$, then $x(t) = 0$ for $t > 0$. By the supposition, we have that

$$x(t) = \sum_{k \in \mathbb{Z}_N} a_{t,k} y_k = 0, \quad -N \leq t \leq N, \quad (9)$$

for some set $\{y_k\}$, where $a_{t,k} = \text{sinc}(k\pi + \Omega m)$; see, e.g., (2). By Theorem 1(a) from [21], the matrix $\{a_{t,k}\}_{k,m=-N}^N \in \mathbf{R}^{2N+1, 2N+1}$ is non-singular. Therefore, linear system (9) is a system with a non-singular matrix. Hence $y_k = 0$ for all k . This proves Lemma 3.1 for the case where $s - q = 2N + 1$.

Let us consider the case where $s - q > 2N + 1$. In this case, the linear system (9) has to be considered jointly with the system

$$\sum_{k \in \mathbb{Z}_N} a_{t,k} y_k = 0, \quad -q \leq t < -N. \quad (10)$$

Clearly, system (9)-(10) admits only a zero solution again. This completes the proof of Lemma 3.1. \square

Proof of Corollary 3.1. Assume first that $s - q = 2N + 1$. Again, we assume that $s = N$. Since homogeneous linear system (9) allows only zero solution, it follows that the non-homogeneous system

$$\sum_{k \in \mathbb{Z}_N} a_{t,k} y_k = x(t_k), \quad -N \leq t \leq N \quad (11)$$

admits a unique solution $\{y_k\}$ for any set $\{x(t_k)\}$. Therefore, we proved that $\{x(t)\}_{t \in \mathcal{T}} \in B_N$ for any $x \in \ell_2$. Further, if $s - q < 2N + 1$, then there are many solutions of (11), and these solutions form a linear manifold. This completes the proof of Corollary 3.1. \square

Consider the mapping $\zeta : \mathbb{B}_N \rightarrow B_N$ such that $x(t) = (\zeta(X))(t) = (\mathcal{Z}^{-1}X)(t)$ for $t \in \mathcal{T}$. It is a linear continuous operator. By Lemma 3.1, it is a bijection.

Proof of Theorem 3.1. The quadratic form here is defined on a finite dimensional linear subspace of $\ell_2(q, s)$. Hence there exists a unique projection \hat{x} of $\{x(t)\}_{t \in \mathcal{T}}$ on B_N , and statement (i) is proven. Statement of Theorem 3.1 (ii) follows from Lemma 3.1. \square

Proof of Corollary 3.2 follows immediately from Corollary 3.1 and Lemma 3.1. \square

Proof of Theorem 3.2. Statement (i) follows from Theorem 1(a) from [21] applied to the matrix $\{\text{sinc}(k\pi + \Omega m)\}_{k,m=-N}^N$. It can be seen from the following. Let $s = N$, $q \leq -N$, $V_0 = \{\text{sinc}(k\pi +$

$\Omega m\}_{k=-N, m=q}^{N, s} \in \mathbf{R}^{2N+1, q-s}$, then $R - V_0 V_0^\top$ is non-negative definite. It follows that R is positively defined. This proves statement (i).

Let us prove statement (ii). Let the Hermitian form $F : B_N \times \mathcal{X}_- \rightarrow \mathbf{R}$ be defined as

$$F(\hat{x}, x) = \|\hat{x} - x\|_{\mathcal{X}_-}^2 = \sum_{t=q}^s |\hat{x}(t) - x(t)|^2.$$

Further, let the Hermitian form $G : \mathcal{Y}_N \times \mathcal{X}_- \rightarrow \mathbf{R}$ be defined as

$$G(y, x) = F(\mathcal{Q}y, x).$$

It follows that

$$G(y, x) = \|\hat{x} - x\|_{\mathcal{X}_-}^2, \quad \hat{x} = \mathcal{Q}y.$$

Clearly, problem (1) can be replaced by the minimization problem

$$\text{Minimize} \quad G(y, x) \quad \text{over} \quad y \in \mathcal{Y}_N.$$

By the definition, it follows that

$$\begin{aligned} G(y, x) &= (\mathcal{Q}y - x, \mathcal{Q}y - x)_{\mathcal{X}_-} = (\mathcal{Q}y, \mathcal{Q}y)_{\mathcal{X}_-} - 2\text{Re}(\mathcal{Q}y, x)_{\mathcal{X}_-} + (x, x)_{\mathcal{X}_-} \\ &= (\mathcal{Q}y, \mathcal{Q}y)_{\mathcal{X}_-} - 2\text{Re}(\mathcal{Q}y, x)_{\mathcal{X}_-} + (x, x)_{\mathcal{X}_-}. \end{aligned}$$

As was mentioned above, it follows from the properties of the sinc function that the mapping $\mathcal{Q}^* : \ell_2 \rightarrow \ell_2$ defined by (3) is continuous, and, therefore, the operator \mathcal{Q}^* can be extended as a continuous linear operator $\mathcal{Q}^* : \mathcal{X}_- \rightarrow \mathcal{Y}_N$. It follows that

$$G(y, x) = (y, Ry)_{\mathcal{Y}_N} - 2\text{Re}(y, \mathcal{Q}^*x)_{\mathcal{Y}_N} + (x, x)_{\mathcal{X}_-},$$

i.e., this is a quadratic form defined on $\mathcal{Y}_N \times \mathcal{Y}_N$. By the definitions, the operator R is non-negative definite, and, by Lemma 3.1,

$$(y, Ry)_{\mathcal{Y}_N} = (\mathcal{Q}y, \mathcal{Q}y)_{\mathcal{X}_-} > 0 \quad \forall y \neq 0_{\mathcal{Y}_N}. \quad (12)$$

Finally, statement (ii) follows from the invertibility of R and the standard properties of the quadratic forms. This completes the proof of Theorem 3.2. \square

Proof of Theorem 3.3. By Theorem 3.2 applied for $q = -\infty$, $s = 0$, x_L is a unique solution of problem (1). In this case, $\mathcal{X}_- = \ell_2(-\infty, s)$. By (12), x_L is a unique solution of problem

$$\text{Minimize} \quad \|x - \mathcal{Q}y\|_{\ell_2(-\infty, s)}^2 \quad \text{over} \quad y \in \ell_2.$$

By the definitions,

$$\|x - \mathcal{Q}y\|_{\ell_2(-\infty, s)}^2 = (y, Ry)_{\ell_2} - 2(y, \mathcal{Q}x_L)_{\ell_2} + (x_L, x_L)_{\ell_2(-\infty, s)}.$$

The value

$$\rho = (x_L, x_L)_{\ell_2(-\infty, s)} - (\mathcal{Q}x_L, R^{-1}\mathcal{Q}x_L)_{\ell_2}$$

represents the optimal value of problem (13). Clearly, x_L is left band-limited if and only if $\rho = 0$. This completes the proof. \square

Proof of Theorem 3.4. By the definition of \mathcal{Q} , for $\hat{X} = \mathcal{Q}y$ and $\hat{x} = \mathcal{Z}^{-1}\hat{X}$, we have that

$$\|\hat{x}\|_{\ell_2}^2 = \frac{1}{2\pi} \|\hat{X}\|_{L_2(-\pi, \pi)}^2 = \|y\|_{\ell_2}^2.$$

Hence problem (7) is equivalent to the problem

$$\text{Minimize } \|\hat{x} - x\|_{\chi_-}^2 + \varepsilon \|y\|_{\ell_2}^2 \quad \text{over } y \in \mathcal{Y}_N, \quad \hat{x} = \mathcal{Q}y. \quad (13)$$

The remaining part of the proof is similar to the proof of Theorem 3.2 with R and $G(y, x)$ replaced by R_ε and $G(y, x) + \varepsilon \|y\|_{\ell_2}^2$ respectively. \square

5 Some numerical experiments

We did some numerical experiments to compare statistically the performance of our band-limited extrapolations with extrapolations based on splines applied to causally smoothed processes.

5.1 Simulation of the input processes

The setting of Theorems 3.2 does not involve stochastic processes and probability measure; it is oriented on extrapolation of real sequences. However, to provide sufficiently large sets of input sequences for statistical estimation, we used processes x generated via Monte-Carlo simulation as a stochastic process evolving as

$$z(t) = A(t)z(t-1) + \sigma\eta(t), \quad t \in \mathbb{Z}, \quad x(t) = c^\top z(t).$$

Here $z(t)$ is a process with the values in \mathbf{R}^ν , where $\nu \geq 1$ is an integer, $c \in \mathbf{R}^\nu$. The process η represents a noise with values in \mathbf{R}^ν , $A(t)$ is a matrix with the values in $\mathbf{R}^{\nu \times \nu}$ with the spectrum inside \mathbb{T} , $\sigma > 0$. The matrices $A(t)$ are switching values randomly at random times; this replicates a situation where the parameters of a system cannot be recovered from the observations such as described in the review [23].

In each simulation, we selected random and mutually independent $(\nu, \sigma, z(-N), A(\cdot), \eta)$, with vectors and matrices having mutually independent components. We selected $\nu \in \{1, \dots, 10\}$ randomly with equal probability, and we selected σ from the uniform distribution on the interval $(0, 2)$. The process η was selected as a stochastic discrete time Gaussian white noise with the values in \mathbf{R}^ν such that $\mathbf{E}\eta(t) = 0$ and $\mathbf{E}|\eta(t)|^2 = 1$. The initial vector $z(-N)$ was selected randomly with the

components from the uniform distribution on $(0, 1)$. The components of the matrix $A(-N)$ was selected from the uniform distribution on $(0, 1/\nu)$. Further, to simulate randomly changing $A(t)$, a random variable ξ distributed uniformly on $(0, 1)$ and independent on $(A(s)|_{s < t}, \eta, z(-N))$ was simulated for each time $t > -N$. In the case where $\xi < 0.5$, we selected $A(t) = A(t-1)$. In the case where $\xi \geq 0.5$, $A(t)$ was simulated randomly from the same distribution as $A(-N)$, independently on $(A(s)|_{s < t}, \eta, z(-N))$. This setting with randomly changing $A(t)$ makes impossible to identify the parameters of equation (14) from the current observations.

5.2 Comparison of band-limited extrapolation with spline extrapolations

We compared root-mean-square errors (RMSEs) for the forecasting via extrapolations of the band-limited approximation obtained in Theorem 3.2 with the RMSEs of standard some spline extrapolations.

We denote below by \mathbb{E} the sample mean across the Monte Carlo trials.

We estimate the root-mean-square error (RMSE) for the forecasting

$$e_{BL} = \mathbb{E} \left[\left(\sum_{t=q+1}^{q+L} |x(t) - \hat{x}_{BL}(t)|^2 \right)^{1/2} \right], \quad (14)$$

given that the extrapolation of the band-limited approximation is accepted as the forecast. Here \hat{x}_{BL} is an extrapolation on future times $t = q + 1, q + 2, \dots, q + L$ of the band-limited approximation described in Theorem 3.2 for the underlying process $x|_{t=q, \dots, s}$ with R replaced by $R_\varepsilon = R + \varepsilon I$, in the terms of this theorem. The choice of integers $L > 0$ defines the forecasting horizon.

We have compared these values with similar values obtained for some standard spline extrapolations of the causal h -step moving average process for x . More precisely, to take into the account truncation, we used a modification of the causal moving average

$$x_{MA}(t) = \frac{1}{\min(h, t + N + 1)} \sum_{k=\max(t-h, -N)}^t x(k), \quad t \geq -N.$$

For three different types of standard spline extrapolations, we calculated the root-mean-square error (RMSE)

$$e_{spline} = \mathbb{E} \left[\left(\sum_{t=1}^L |x(t) - x_{spline}(t)|^2 \right)^{1/2} \right], \quad (15)$$

given that the spline is accepted as the forecast. Here x_{spline} is a spline extrapolation of the observed moving average $x_{MA}|_{t=q, \dots, s}$. We considered the the piecewise cubic extrapolation, the shape-preserving piecewise cubic extrapolation, and the linear extrapolation. We used built in MATLAB code *interp1* for calculation of these extrapolations.

We used smoothed moving average process x_{MA} as inputs because we found that applications directly to the original "noisy" process x produces quite unsustainable extrapolation with large errors e_{spline} .

We calculated and compared e_{BS} and e_{spline} . Table 5.1 shows the ratios e_{BL}/e_{spline} for some combinations of parameters. For these calculations, we used $c = (1/\nu, 1/\nu, \dots, 1/\nu)^\top$, $h = 10$, and $\varepsilon = 0.1$.

5.3 Impact of preliminary smoothing

It is common to apply a forecasting method to processes that are preliminary smoothed by a causal filter. For many methods, it helps to improve performance. We did some experiments to investigate the impact of this smoothing on relative performance of the band-limited extrapolation and spline extrapolation. We repeated experiments described above with the following modification: we calculated band-limited projections and their extrapolations for the causally smoothed process $x_{MA}(t)$, and compared the performance of the corresponding predictor with the performance of defined by the same spline extrapolations and applied to x_{MA} as described above. Again, we calculated and compared corresponding RMSEs e_{BL} and e_{spline} , with $c = (1/\nu, 1/\nu, \dots, 1/\nu)^\top$, $h = 10$, $s = 0$, $q = -150, -70$, and $\varepsilon = 0.1$. Table 5.2 shows the ratios e_{BL}/e_{spline} for some combinations of parameters with $s = 0$ and $q = -150, -70$.

Comparing Tables 5.1 and 5.2, we observe that using smoothed moving average process x_{MA} instead of the original process x as the input for the band-limited approximation and extrapolation leads to slightly increased ratios e_{BL}/e_{spline} . Since the errors e_{spline} used for Table 5.2 are the same as the ones used for Table 5.1, it follows that the errors e_{BL} are slightly larger with the smoothed moving average process x_{MA} is used instead of the original process x as the input for the left band-limited approximation and extrapolation. The fact that a preliminary smoothing does not improve performance of the suggested left band-limited smoothing speaks in favor of our method. This is expected for filters targeting approximation of an ideal low-pass filter, because moving average damps higher frequency but distorts significantly a signal characteristics on a wider spectrum.

5.4 Discussion of the results of the experiments

The experiments demonstrated a good numerical stability of the method; the results were quite robust with respect to truncation of the input processes and deviations of parameters. For each entry in Tables 5.1-5.2, we used 30,000 Monte-Carlo trials; increasing or decreasing the number of Monte-Carlo trials also gives very close results. For instance, an experiment with 60,000 Monte-Carlo trials produced the set of results (0.9834, 0.6436, 0.1426, 0.0459) for the last row of Table 5.2. An experiment with 15,000 Monte-Carlo trials produced the set of results (0.8508, 0.2378, 0.0530, 0.0194) for the 3rd row of Table 5.1.

Table 5.1: The ratios of root-mean-square errors e_{BL}/e_{spline} defined by (14)-(15) for band-limited extrapolation of $x|_{q \leq t \leq 0}$ and spline extrapolations of $x_{MA}|_{q \leq \theta \leq 0}$.

| Type of spline extrapolation | e_{BL}/e_{spline} | | | |
|------------------------------------|------------------------|---------|---------|----------|
| | Extrapolation horizons | | | |
| | $L = 1$ | $L = 4$ | $L = 8$ | $L = 12$ |
| $\Omega = \pi/4, N = 50, q = -150$ | | | | |
| Linear | 0.8900 | 0.8825 | 0.7781 | 0.6742 |
| Piecewise cubic | 0.8429 | 0.2359 | 0.052 | 0.0192 |
| Shape-preserving piecewise cubic | 0.9001 | 0.6303 | 0.1414 | 0.0448 |
| $\Omega = \pi/2, N = 30, q = -70$ | | | | |
| Linear | 0.9010 | 0.9005 | 0.7840 | 0.6837 |
| Piecewise cubic | 0.8675 | 0.2408 | 0.0530 | 0.0193 |
| Shape-preserving piecewise cubic | 0.9082 | 0.6475 | 0.1436 | 0.0464 |

The ratios e_{BL}/e_{spline} are decreasing further as the horizon L is increasing, hence we omitted the results for $L > 12$. By the same reasons, we omitted results with classical extrapolations applied directly to $x(t)$ instead of the moving average $x_{MA}(t)$, since the distance (15) is quite large in this case due the presence of the noise.

Figure 5.1 shows examples of paths $x(t)$, their band-limited causal approximation and extrapolation \hat{x}_{BL} , with the same parameters as were used for Tables 5.1. These figures also show the moving averages $x_{MA}(t)$, and their spline extrapolations $x_{spline}(t)$.

Figure 5.2 shows examples of paths $x(t)$, the moving averages $x_{MA}(t)$, the band-limited causal approximation and extrapolation \hat{x}_{BL} obtained for $x_{MA}(t)$, with the same parameters as were used for Tables 5.2. The figure also shows spline extrapolations $x_{spline}(t)$ of x_{MA} .

6 Possible applications and future development

The approach suggested in this paper allows many modifications. We outline below some possible straightforward modifications as well as more challenging problems and possible applications that we leave for the future research.

1. The mean-square optimal causal band-limited approximations of one-sided sequences suggested above can be interpreted as outputs causal smoothing filter. To accommodate the

Table 5.2: The ratios of root-mean-square errors e_{BL}/e_{spline} defined by (14)- (15) for band-limited extrapolation of the moving average $x_{MA}|_{q \leq t \leq 0}$ and spline extrapolations of $x_{MA}|_{q \leq \theta \leq 0}$.

| Type of spline extrapolation | e_{BL}/e_{spline} | | | |
|----------------------------------|------------------------------------|---------|---------|----------|
| | Extrapolation horizons | | | |
| | $L = 1$ | $L = 4$ | $L = 8$ | $L = 12$ |
| | $\Omega = \pi/4, N = 50, q = -150$ | | | |
| Linear | 0.9891 | 0.8915 | 0.7719 | 0.6677 |
| Piecewise cubic | 0.9464 | 0.2425 | 0.0536 | 0.0196 |
| Shape-preserving piecewise cubic | 0.9882 | 0.6490 | 0.1446 | 0.0468 |
| | $\Omega = \pi/2, N = 30, q = -70$ | | | |
| Linear | 0.9736 | 0.8934 | 0.7785 | 0.6777 |
| Piecewise cubic | 0.9362 | 0.2416 | 0.0530 | 0.0193 |
| Shape-preserving piecewise cubic | 0.9783 | 0.6531 | 0.1459 | 0.0472 |

current flow of observations, the coefficients of the sinc series have to be changed dynamically; therefore, the corresponding filter is not time invariant. It can be noted that, for some problems, time invariance for a filter is not crucial. For example, a typical approach to forecasting in finance is to approximate the known path of the stock price process by a process that has a unique extrapolation that can be used as a forecast. This procedure can be done at current time; it is not required that the same forecasting rule will be applied at future times.

- Tables 5.1-5.2 show that the band-limited extrapolation performs better than the spline extrapolations; some additional experiments with other choices of parameters demonstrated the same trend. However, experiments did not involve more advanced methods beyond the listed above spline methods. Nevertheless, regardless of the results of these experiments, potential importance of band-limited extrapolation is self-evident because its physical meaning: a band-limited part can be considered as a regular part of a process purified from a noise represented by high-frequency component. This is controlled by the choice of the band. On the other hand, the choice of particular splines does not have a physical interpretation.
- The set $\{e^{i\omega}, \omega \in [-\Omega, \Omega]\} \subset \mathbb{T}$ can be replaced by another set, for example, by a set that is not necessarily connected, in a setting that is close to one from [15]. This would require a minor modification of the algorithm.

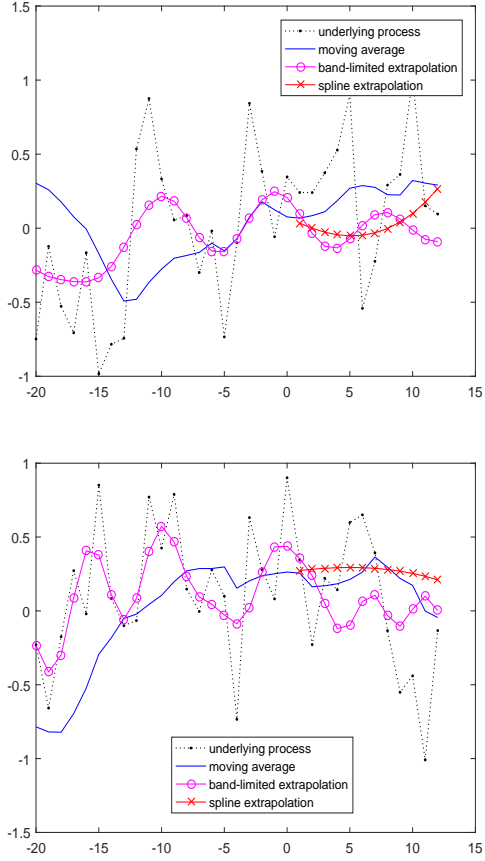


Figure 5.1: Example of a path $x(t)$, its moving average x_{MA} , the band-limited causal approximation and extrapolation \hat{x}_{BL} of $x|_{t \leq 0}$, and shape-preserving piecewise cubic extrapolation x_{spline} of $x_{MA}|_{t \leq 0}$, with $\Omega = \pi/4$, $N = 50$, $q = -150$, $s = 0$, $h = 10$, $\varepsilon = 0.1$ (top) and $\Omega = \pi/2$, $N = 30$, $q = -70$, $s = 0$, $h = 10$, and $\varepsilon = 0.1$ (bottom).

4. It is possible to consider a setting where some observations of the past values $x(t)$ are missing.
5. Instead of Fourier series, expansion by another basis in $L_2(-\Omega, \Omega)$ can be used, for instance, such as suggested in [24]. The space $L_2(-\Omega, \Omega)$ can be replaced by a weighted L_2 -spaces, for a weight representing a relative importance of the approximation on different frequencies.

Acknowledgements

This work was supported by ARC grant of Australia DP120100928 to the author.

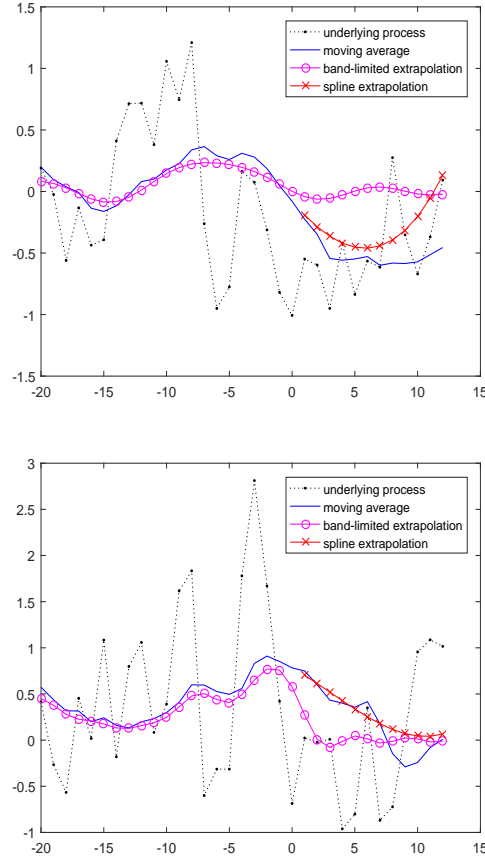


Figure 5.2: Example of a path $x(t)$, its moving averages $x_{MA}(t)$, the band-limited causal approximation and extrapolation \hat{x}_{BL} of $x_{MA}|_{t \leq 0}$, and shape-preserving piecewise cubic extrapolation x_{spline} of $x_{MA}|_{t \leq 0}$ with $\Omega = \pi/4$, $N = 50$, $q = -150$, $s = 0$, $h = 10$, $\varepsilon = 0.1$ (top) and $\Omega = \pi/2$, $N = 30$, $q = -70$, $s = 0$, $h = 10$, and $\varepsilon = 0.1$ (bottom).

References

- [1] Aldroubi, A., and Unser, M. A general sampling theory for nonideal acquisition devices. (1994). *IEEE Trans. Signal Process.*, Vol.42, No. 11 2915–2995.
- [2] Alem, Y., Khalid, Z., Kennedy, R.A. (2014). Band-limited extrapolation on the sphere for signal reconstruction in the presence of noise, *Proc. IEEE Int. Conf. ICASSP'2014*, pp. 4141-4145.
- [3] Almira, J.M. and Romero, A.E. (2008). How distant is the ideal filter of being a causal one? *Atlantic Electronic Journal of Mathematics* **3** (1) 46–55.
- [4] Bingham, N. H. (2012). Szegő's theorem and its probabilistic descendants. *Probability Surveys* **9**, 287-324.

- [5] Butzer, P.L. and Stens R.L. (1993). Linear prediction by samples from the past. In: *Advanced Topics in Shannon Sampling and Interpolation Theory* (R.J. Marks II, ed.), Springer-Verlag, New York, 1993, pp. 157-183.
- [6] Candés E., Tao, T. (2006), Near optimal signal recovery from random projections: Universal encoding strategies? *IEEE Transactions on Information Theory* **52**(12) (2006), 5406-5425.
- [7] Candes, E.J., J Romberg,J., Tao, T. (2006). Robust uncertainty principles: Exact signal reconstruction from highly incomplete frequency information *IEEE Transactions on Information Theory* **52** (2), 489–509.
- [8] Cambanis, S., and Soltani, A.R. (1984). Prediction of stable processes: spectral and moving average representations. *Z. Wahrsch. Verw. Gebiete* **66**, no. 4, 593–612.
- [9] Dokuchaev, N. (2010). Predictability on finite horizon for processes with exponential decrease of energy on higher frequencies, *Signal processing* **90** (2) (2010) 696–701.
- [10] Dokuchaev, N. (2012a). On predictors for band-limited and high-frequency time series. *Signal Processing* **92**, iss. 10, 2571-2575.
- [11] Dokuchaev, N. (2012b). Predictors for discrete time processes with energy decay on higher frequencies. *IEEE Transactions on Signal Processing* **60**, No. 11, 6027-6030.
- [12] Dokuchaev, N. (2012c). On sub-ideal causal smoothing filters. *Signal Processing* **92**, iss. 1, 219-223.
- [13] Dokuchaev, N. (2016). Near-ideal causal smoothing filters for the real sequences. *Signal Processing* **118**, iss. 1, pp. 285-293.
- [14] Dokuchaev, N. (2017). On detecting predictability of one-sided sequences. *Digital Signal Processing* **62**, pp. 26–29.
- [15] Ferreira P. G. S. G. (1994). Interpolation and the discrete Papoulis-Gerchberg algorithm. *IEEE Transactions on Signal Processing*, **42** (10), 2596–2606.
- [16] Ferreira P. G. S. G.. (1995a). Nonuniform sampling of nonbandlimited signals. *IEEE Signal Processing Letters* **2**, Iss. 5, 89–91.
- [17] Ferreira P. G. S. G.. (1995b). Approximating non-band-limited functions by nonuniform sampling series. In: *SampTA '95, 1995 Workshop on Sampling Theory and Applications*, 276–281.
- [18] Ferreira P. J. S. G., Kempf A., and Reis M. J. C. S. (2007). Construction of Aharonov-Berrys superoscillations. *J. Phys. A, Math. Gen.*, vol. 40, pp. 5141–5147.

- [19] Jerri, A. (1977). The Shannon sampling theorem - its various extensions and applications: A tutorial review. *Proc. IEEE* **65**, 11, 1565–1596.
- [20] Kolmogorov, A.N. (1941). Interpolation and extrapolation of stationary stochastic series. *Izv. Akad. Nauk SSSR Ser. Mat.*, 5:1, 3–14.
- [21] Lee, D.G., Ferreira, P.J.S.G. (2014). Direct construction of superoscillations. *IEEE Transactions on Signal processing*, V. 62, No. 12, 3125–3134.
- [22] Rudin, W. *Real and Complex Analysis*. 3rd ed. Boston: McGraw-Hill, 1987.
- [23] Smith, D.A., William F. Ford, W.F., Sidi, A. (1987). Extrapolation methods for vector sequences *Siam Review*, vol. 29, no. 2, 199–233.
- [24] Tzschope, R. and Huber, J. B. (2009), Causal discrete-time system approximation of non-bandlimited continuous-time systems by means of discrete prolate spheroidal wave functions. *Eur. Trans. Telecomm.***20**, 604–616.
- [25] Wiener, N. (1949). *Extrapolation, Interpolation, and Smoothing of Stationary Time Series with Engineering Applications*, Technology Press MIT and Wiley, New York.
- [26] Yosida, K. (1965). *Functional Analysis*. Springer, Berlin Heilderberg New York.
- [27] Zhao, H., Wang, R., Song, D., Zhang, T., Wu, D. (2014). Extrapolation of discrete bandlimited signals in linear canonical transform domain. *Signal Processing* **94**, 212–218.
- [28] Zhao, H., Wang, R., Song, D., Zhang, T., Liu, Y. (2014). Unified approach to extrapolation of bandlimited signals in linear canonical transform domain. *Signal Processing* **101**, 65–73.